Computational Materials Science 87 (2014) 76–82

Contents lists available at ScienceDirect

Computational Materials Science

journal homepage: www.elsevier.com/locate/commatsci

Atomistic simulation of single crystal copper nanowires under tensile stress: Influence of silver impurities in the emission of dislocations

N. Amigo [a,*], G. Gutiérrez [a], M. Ignat [b]

[a] Grupo de NanoMateriales, Departamento de Física, Facultad de Ciencias, Universidad de Chile, Casilla 653, Santiago, Chile
[b] Departamento de Física y de Ingeniería Mecánica, Facultad de Ciencias Físicas y Matemáticas, Universidad de Chile, Santiago, Chile

ARTICLE INFO

Article history:
Received 26 September 2013
Received in revised form 4 February 2014
Accepted 8 February 2014

Keywords:
Molecular dynamics
Tensile test
Impurities
Dislocations

ABSTRACT

The transition from elastic to plastic behaviour in single crystal copper nanowires under uniaxial tensile stress at different concentrations of silver (0.0–0.5 at.% Ag) and at different temperatures (0.1, 100, and 300 K) using the molecular dynamics method is investigated. The tensile stress is applied along ⟨100⟩ crystallographic orientation and the silver atoms are placed randomly on the surface of the nanowire, as substitutional point defect. The simulations indicate that silver atoms lower slightly the unstable stacking fault energy, making them act as sources of partial dislocation nucleation, due to the local strain field they produce in the lattice structure. The defects generated in the material also act as sources for nucleation, giving rise to a competition of two mechanism. Also, it is observed that the yield point decreases with the temperature and the presence of impurities.

1. Introduction

Electronic devices are getting smaller from year to year in the last decade, reaching molecular levels. Thus, materials with good mechanical properties and electrical conductivity are required. The unusual electrical behaviour of metallic nanowires make them a material of interest in such area [1–6], increasing their importance. Studies on the mechanical properties are necessary to understand the behaviour of the nanowires in their different applications. In the recent years, different research regarding mechanical properties of materials using computational techniques have been carried out, such as dislocation nucleation [7,8], grain size effects [9,10], void growth and them serving as crack seed [11–14], surface defects [15], among many others. In most cases the crystal structure of materials are not defect free, so imperfections, such as vacancies, impurities, and grain boundaries are needed to be included in the studies. However, to our knowledge, there is limited information about the effects of impurities on the mechanical properties of metals using computational simulation [16–19], making necessary studies which describe the influence of this kind of defect on the mechanical properties of the material.

In the present work, we study the influence of silver impurities on the partial dislocations nucleation, analysing its effect on the unstable stacking fault energy of copper. Also, the yield point of copper nanowires with silver impurities at different concentration levels (from 0.0 to 0.5 at.% Ag) and at different temperatures (0.1, 100, and 300 K) is investigated. We use the molecular dynamics method, submitting the system to uniaxial tensile stress.

The paper is organized as follows: In Section 2 we explain the simulation procedure used and the tools for analysis employed, in Section 3 we present and discuss our results, and in Section 4 we draw the conclusions.

2. Methodology

The system under study consists of a face centred cubic (fcc) copper nanowire with square cross-section, like most nanowires studied in previous works [20–23], with a size corresponding to $40 \times 10 \times 10$ in terms of the lattice parameter, which is 3.61 Å for copper. The orientation is such that the axial axis is along [100] direction, with six {100} side surfaces, as is shown in Fig. 1. Free boundary conditions are imposed in all directions. Different silver impurity concentrations (0.0–0.5 at.% Ag) are added on the surface as substitutional defects, since it is well-known that silver segregates to Cu grain boundaries and surfaces [24–26] due to its limited solubility [27] (in Fig. 1 blue atoms represent copper and the red ones silver). The procedure to create the different impurity concentration systems is straightforward. First, a concentration of 0.1 at.% Ag is placed randomly on the surface of the impurity free nanowire, obtaining the Cu 0.1 at.% Ag system. Thus,

* Corresponding author.
E-mail addresses: nicorafa@gmail.com (N. Amigo), gonzalo@fisica.ciencias.uchile.cl (G. Gutiérrez).

http://dx.doi.org/10.1016/j.commatsci.2014.02.014
0927-0256/

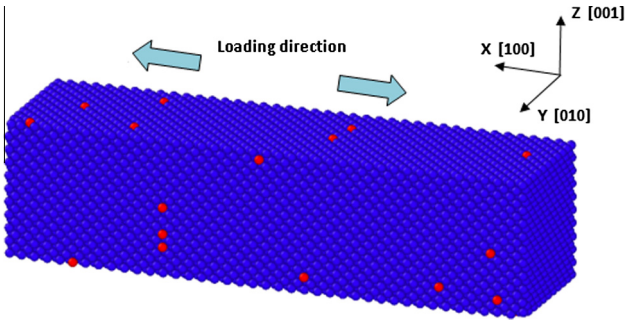

Fig. 1. Initial configuration of the copper nanowire. Copper and silver atoms are represented by blue and red color, respectively. The loading of the system is along the axial direction, which lies in the [100] direction. (For interpretation of the references to color in this figure legend, the reader is referred to the web version of this article.)

a particular realization of this system is created. Then, a concentration of 0.1 at.% Ag is added, again randomly, on the surface of this system, thus obtaining the Cu 0.2 at.% Ag system. This procedure is repeated three more times in order to obtain the Cu 0.3, 0.4 and 0.5 at.% Ag systems.

The simulation is carried out using the classical molecular dynamics code LAMMPS developed by Plimpton et al. at Sandia National Laboratories [28] and the visualization by means of OVITO [29]. The inter-atomic potential employed for copper-silver alloys is the well established embedded-atom method (EAM) potential developed by Williams et al. [30] which is based on the previous potential developed by Mishin et al. for Cu [31]. In general, the EAM gives the total energy of an atomic system in the form [32]

$$E = \frac{1}{2}\sum_{ij} V_{ij}(r_{ij}) + \sum_{i} F_i(\bar{\rho}_i), \tag{1}$$

where E is the total energy of the system, and V_{ij} is the pair potential between atoms i and j separated by a distance r_{ij}. F_i is the energy of atom i embedded in an electron density $\bar{\rho}_i$, given by

$$\bar{\rho}_i = \sum_{i \neq j} \rho_j(r_{ij}). \tag{2}$$

The quantity $\rho_j(r_{ij})$ represents the electron density at atom j as function of the distance r_{ij}.

The procedure of the simulation is the following. First, the energy of the system is minimized using conjugate gradient method. Then, a thermalization at 0.1 K, 100 K or at 300 K (depending on the temperature wanted to be studied), is performed using velocity rescaling for 10 ps, using 1 fs as the integration time step. After this procedure, the system is loaded along the axial direction at a strain rate of 10^8 s^{-1}. For this purpose, the positions of atoms are rescaled each time step. The temperature is kept constant during the tensile process in order to avoid thermal effects related to dislocation propagation.

The stress in the system is calculated from the stress tensor expression as implemented in LAMMPS [28]

$$\sigma_{ij} = -\frac{1}{V}\sum_{\alpha}\left(m^{\alpha} v_i^{\alpha} v_j^{\alpha} + \frac{1}{2}\sum_{\beta \neq \alpha} r_i^{\alpha\beta} F_j^{\alpha\beta}\right), \tag{3}$$

where V is the volume of the system, m^{α} is the mass of atom α, v_i^{α} and v_j^{α} are the i and j-component of velocity respectively, $F_i^{\alpha\beta}$ is the i-component of the force between atom α and β, and $r_j^{\alpha\beta}$ is the j-component of the distance between atom α and β. The first term is associated with the kinetic energy due to thermal vibration and the second term with the potential energy due to the deformation of the system. Note that since the loading is in the (100) axial direction, only the σ_{ii} stress component is required.

To study the partial dislocation nucleation and stacking faults in the system, the centrosymmetry parameter (CSP) [33] is used, which is defined for a particular atom i as

$$c_i = \sum_{j=1}^{N/2} \left| \vec{R}_j + \vec{R}_{j+\frac{N}{2}} \right|^2, \tag{4}$$

where N is the number of nearest neighbours of atom i, $\vec{R}_j$ and $\vec{R}_{j+\frac{N}{2}}$ are the vectors from the atom to a pair of opposite nearest neighbours. Note that for a face centred cubic structure $N = 12$. The CSP value is zero for atoms in a perfect lattice and it increases for any defects and atoms close to the free surface. In this study, $3.7 < c_i < 4.5$ represents a partial dislocation, $4.5 < c_i < 6.5$ corresponds to stacking fault and $c_i > 6.5$ for free surface.

3. Results and discussion

The stress–strain curves for the six copper nanowires (0.0, 0.1, 0.2, 0.3, 0.4, 0.5 at.% Ag) at 0.1 K are shown in Fig. 2 [34]. As it can be seen, three main features are clearly distinguishable. Firstly, the elastic regimen of the systems is essentially the same, thus the stiffness is almost unaffected by the impurities at the considered concentration levels. Secondly, both the yield stress and yield strain change with the concentration of impurities. Thirdly, after the yield point, a sawtooth behaviour of the curve is observed. This is indicative of a successive emission of dislocations.

3.1. Reduction of the yield point and emission of dislocations

Table 1 presents the calculated values of the yield strain and yield stress for each system. The change of the yield point according to the presence of impurities can be rationalizes in terms of the local strain field generated in the lattice due to the size mismatch

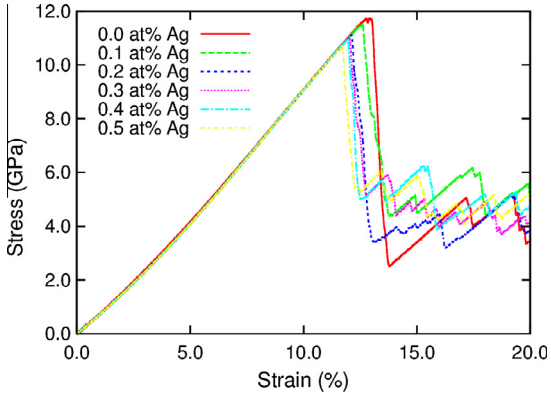

Fig. 2. Stress–strain relationships for single crystal Cu nanowire along [100] direction at different concentrations levels of Ag.

Table 1
Yield strain and yield stress for different concentrations of Ag.

Ag content (at.%)	Yield strain (%)	Yield stress (GPa)
0.0	12.9	11.7
0.1	12.6	11.5
0.2	12.0	11.1
0.3	11.9	11.0
0.4	11.8	10.9
0.5	11.6	10.7

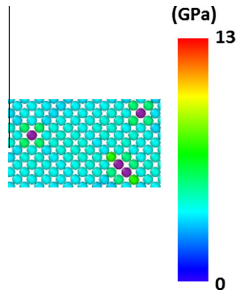

Fig. 3. Von Mises stress distribution in a portion of system surface. The four Ag impurities are the purples ones, which create a higher local stress field around them.

between Ag and Cu atoms (radius difference around 11.5%). In fact, Fig. 3 shows the von Mises stress distribution in a portion of the surface of the initial system, where the silver atoms are in purple. As is well-known, surface atoms have non-zero stress, but clearly the four silver atoms create a higher stress field around them. Thus, impurities are expected to act as sources of partial dislocation nucleation.

To investigate further the decrease of the yield points according the Ag impurities concentration increases, we use the centrosymmetry parameter. The idea is to detect the site where the first partial dislocation is emitted. Thus, using corresponding CSP values, we erase all atoms on the surface and in non-defect regions, except those that belong to partial dislocations, stacking faults and impurities. Fig. 4 displays the onset of plastic deformation in the Cu 0.2 at.% Ag sample. Fig. 4(a) shows the system just before the yield point, at $\epsilon = 11.9\%$ strain. Immediately after that, the first partial dislocation (Shockley partial) is nucleated from a silver atom, crossing the system along the (1 1 1) slip plane and leaving a stacking fault, as it is seen in Fig. 4(b), at $\epsilon = 12.1\%$ strain. In Fig. 4(c), which is a zoom of this stacking fault, can be distinguished the silver atom where the first partial dislocation is nucleated and emitted. The emission of this dislocation induces the first drop in the stress–strain curve, which corresponds to the yield point.

After that, as the sample is continuously stretched, new dislocations are emitted, in correspondence to the other drops in the stress–strain curve. In this way, at strain $\epsilon = 12.3\%$, a second partial dislocation is nucleated, but this time from the step generated by the first partial dislocation, as is shown in Fig. 5(a). Thus, from now on, a competition between the surface and the impurities as nucleation sources begins. Of course, this situation is nothing more than an energy trade off between the cost to create a dislocation from a defective surface or from an impurity atom. Furthermore, as the loading continues, several partial dislocations are nucleated from these two sources and multiple stacking faults, contained in {1 1 1} slip planes, are left in the system, as is shown in Fig. 5(b) at $\epsilon = 12.9\%$ strain. Atoms are coloured according to CSP in a range from 4 to 7 for more clarity.

The same picture emerges for the systems at different Ag concentration. In Fig. 6(a) is presented the first partial dislocation nucleated in the Cu 0.5 at.% Ag, at $\epsilon = 11.7\%$. The second partial is nucleated again from a step produced in the surface by the stacking fault left for the first dislocation, as shown in Fig. 6(b). Similar to the previous Cu 0.2 at.% Ag sample, the first partial is nucleated at impurities, in this case from two silver atoms, as shown in Fig. 6(c). The details for the rest of systems (namely, at concentration 0.1, 0.3, and 0.4 at.% Ag) studied are not commented here, because the mechanism is essentially the same as the already depicted.

3.2. The onset of plasticity and the generalized stacking fault energy curve

The partial dislocations and stacking faults generated in the copper nano-wires along ⟨1 0 0⟩ loading direction presented above are basically the same as those found for pure copper nanowires in previous studies [22]. However, silver impurities affect the stress needed for the nucleation of these defects, modifying the yield point of the material. The main hypothesis stated to explain this behaviour is that the local stress field of the impurities seems to promote partial dislocation nucleation, helping the onset of the plastic deformation. Interestingly, this statement can be tested and quantitatively evaluated. An useful parameter to quantify this effect is the unstable stacking fault energy, γ_{usf}, which gives an estimation on the easiness to nucleate and propagate a dislocation. It can be obtained from the generalized stacking fault energy (GSF) curve [35].

In order to calculate the generalized stacking fault energy curve for copper, two semi-infinite blocks are sheared on a (1 1 1) plane along the [1 1 2] direction, using molecular static technique, as

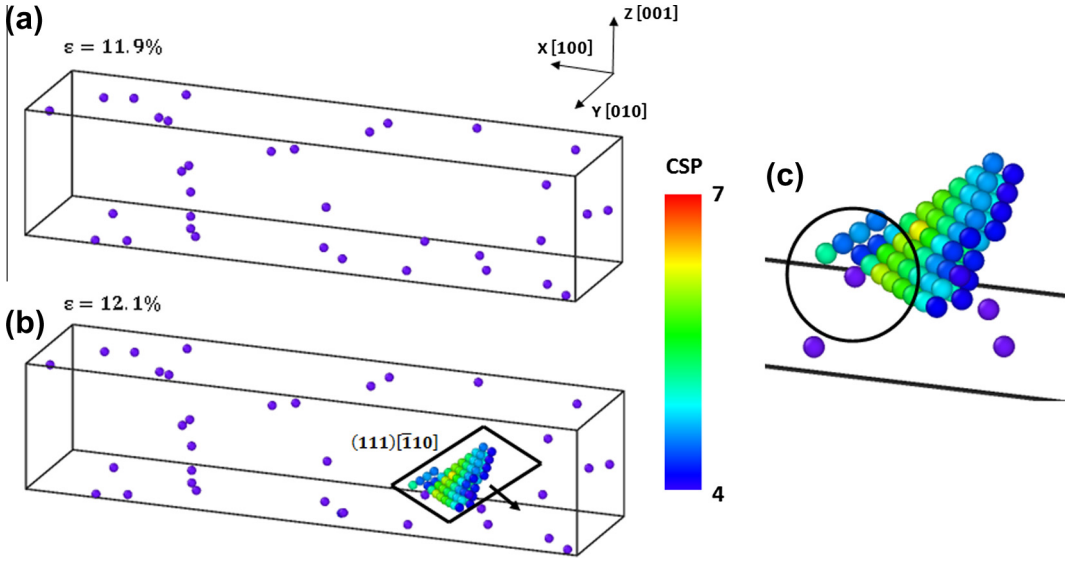

Fig. 4. (a) Cu 0.2 at.% Ag system prior to yielding. Silver atoms are in purple and non-defect fcc Cu atoms has been erased. (b) First partial dislocation emitted in (1 1 1) [1̄ 1 0] followed by the creation of a stacking fault. (c) Inset of the silver atom, enclosed by the black circle, where the first dislocation is nucleated. Atoms are coloured according to CSP. (For interpretation of the references to color in this figure legend, the reader is referred to the web version of this article.)

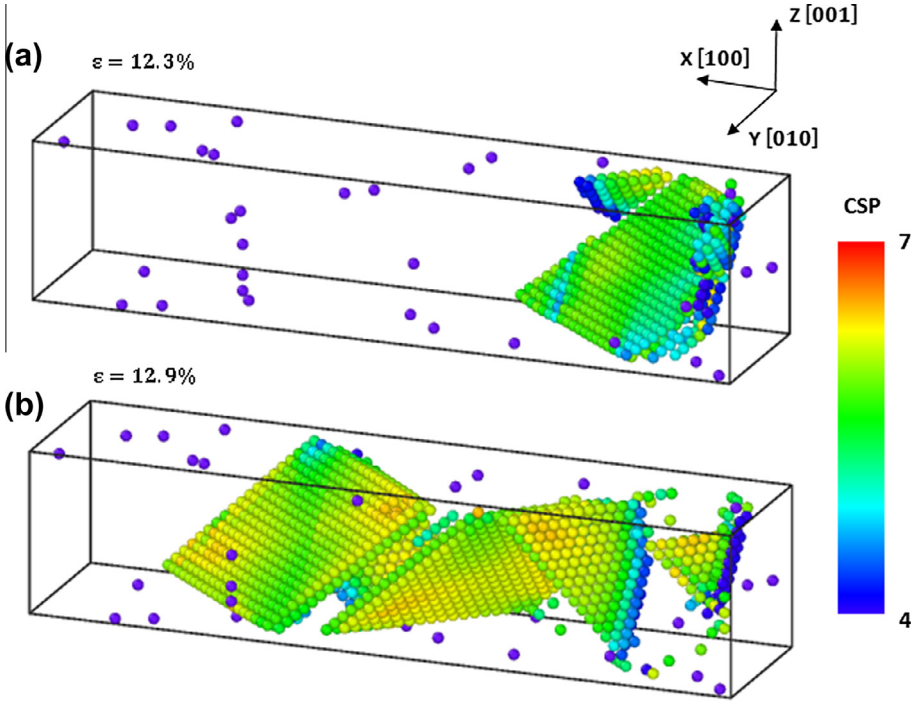

Fig. 5. (a) Second partial dislocation emitted from the step previously generated in Cu 0.2 at.% Ag system. (b) Multiple stacking faults are generated in the system during loading. Atoms are coloured according to CSP. (For interpretation of the references to color in this figure legend, the reader is referred to the web version of this article.)

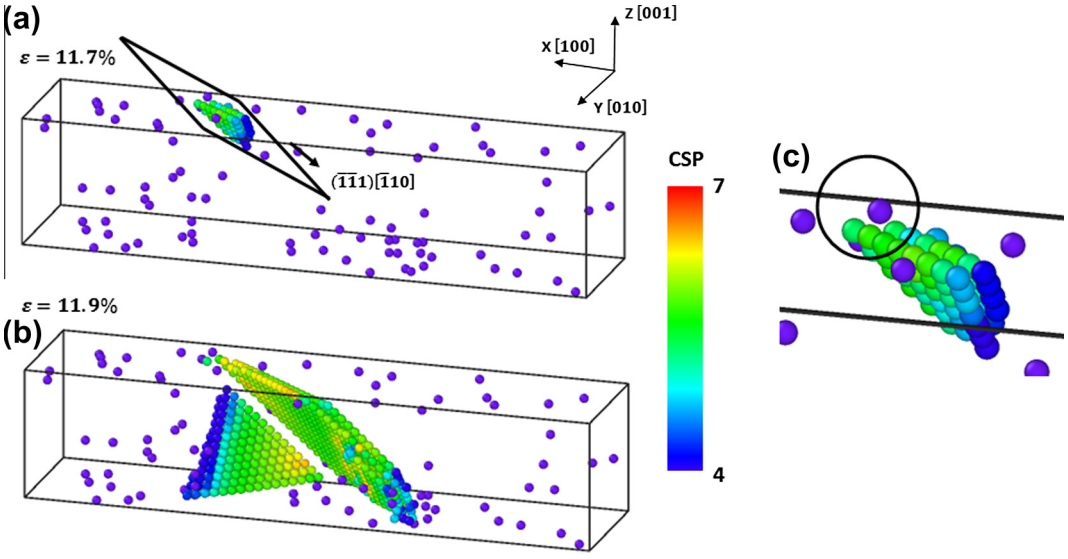

Fig. 6. (a) First partial dislocation emitted in $(\bar{1}\,\bar{1}\,1)$ $[\bar{1}\,1\,0]$ in Cu 0.5 at.% Ag system. (b) The second partial dislocation is nucleated from the step already generated in the system. (c) Inset of the two silver atoms, enclosed by the black circle, where the first dislocation is nucleated. Atoms are colored according to CSP. (For interpretation of the references to color in this figure legend, the reader is referred to the web version of this article.)

showed in Fig. 7. Here the slipping zone (i.e. where the stacking fault will appear) is in red and contains 400 atoms. Periodic boundary conditions are applied in the $[\bar{1}\,1\,0]$ and $[1\,1\,2]$ directions and the system is allowed to relax only in the direction normal to the $(1\,1\,1)$ plane. While the atoms at the upper half are displaced in small increments, the ones at the lower half remain fixed. After each displacement, an energy minimization is performed and the total energy of the system is calculated. This procedure is done for different amounts of silver atoms next to the stacking fault plane (i.e. red atoms in Fig. 7), namely 0, 1, 4 and 8 substitutional silver atoms, obtaining the GSF curve presented in Fig. 8. The unstable stacking fault energy, γ_{usf}, corresponds to the magnitude of the first peak of each GSF curve, and the intrinsic stacking fault energy, γ_{sf}, to the first local minimum beyond the peak, which are summarized in Table 2. Silver impurities reduce the unstable stacking fault energy, although in a small amount, compared to the impurity free system. For example, in the case of one Ag atom next to the stacking fault plane, the decrease in energy is just 0.5 mJ/m^2, but enough to nucleate a dislocation. On the other hand, the intrinsic stacking fault energy remains almost unchanged as the number of Ag atoms increases. Similarly, the effect on the unstable stacking fault energy of an Ag atom, located one atomic

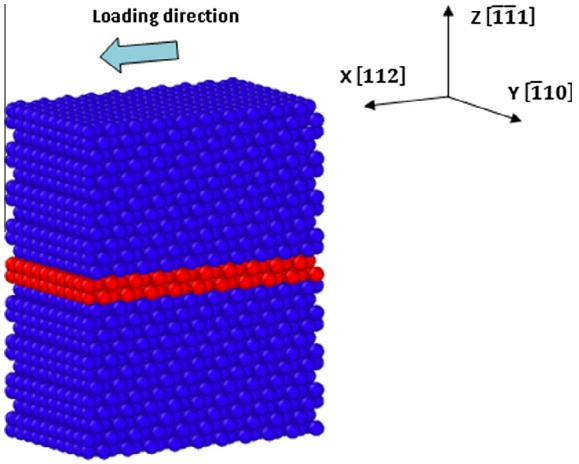

Fig. 7. Initial configuration of bulk copper for the generalized stacking fault energy curve calculation. The red atoms represent the slipping zone. (For interpretation of the references to color in this figure legend, the reader is referred to the web version of this article.)

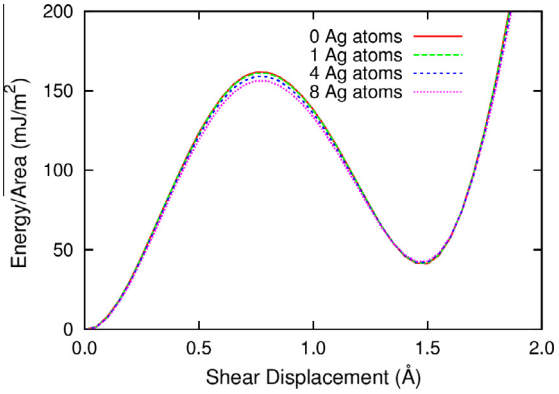

Fig. 8. Generalized stacking fault energy curve for zero, one, four and eight silver atoms next to the stacking fault plane (red, green, blue and purple curve respectively). (For interpretation of the references to color in this figure legend, the reader is referred to the web version of this article.)

Table 2
Unstable (γ_{usf}) and stable (γ_{sf}) stacking fault energies along ⟨1 1 2⟩ direction for different contents of Ag in the slipping zone.

Ag content (number of atoms)	γ_{usf} (mJ/m^2)	γ_{sf} (mJ/m^2)
0	161.7	41.4
1	161.2	41.8
4	159.0	42.2
8	156.2	42.8

plane away from the slipping zone, is negligible: the energy only increases by 0.16 mJ/m^2. Thus, according the changes in energy, the presence of impurities are only noticeable at the beginning of the stretching process, when the sample is still a defect-free system (aside the Ag impurities). After the first stacking fault appears, a defective surface (with a step for example) plays a similar role to an impurity, and these two mechanisms (surface and silver impurities) compete for partial dislocation nucleation. Interestingly, in previous studies on the decrease of the yield point in Cu–Sb single crystal alloys by Rajgarhia et al. [18], it was showed that one antimony atom next to the fault plane lowers γ_{usf} by 6.1 mJ/m^2. Although this reduction is more noticeable than our case of Ag, qualitatively both results are the same. Since these two elements behave as substitutional impurities in copper, it may be expected that the similar behaviour will be found for other substitutional impurities in copper.

3.3. Stress–strain relationships for other Cu–Ag system realizations

The stress–strain curve is also calculated for different Cu–Ag system realizations (or samples) at different concentrations (0.0, 0.2, 0.4 at.% Ag) of impurities in order to determine the influence of silver atoms location on the yield strength. The procedure to create these samples is the same as the one explained in Section 2. A concentration of 0.2 at.% Ag is placed randomly on the impurity free nanowire, creating the Cu 0.2 at.% Ag S2 system. Again, a concentration of 0.2 at.% Ag is added randomly on this system, creating the Cu 0.4 at.% Ag S2 system. Two more different samples are obtained by repeating the whole procedure on a impurity free nanowire, which are called the Cu 0.2 at.% Ag S3 and Cu 0.4 at.% Ag S3 systems. Their corresponding stress–strain curves are shown in Fig. 9 and their associated yield strain and stress are shown in Table 3. As it can be seen in the case of the S2 systems, as the concentration of the silver impurities increases, the yield strength of the system decreases, similar to the results obtained in Section 3.1. However, this effect is not observed in the S3 systems. Despite the yield strength of the nanowire decreases when silver atoms are added, its relationship is not monotonic. Nevertheless, from the multiple peaks of the sawtooth behaviour of the Cu 0.4 at.% Ag S3 curve, it can be noted that its plastic regime is governed by more dislocation emissions than the plastic regime of the Cu 0.2 at.% Ag S3 system. This can be understood by considering the impurity atoms. Since the 0.4 at.% Ag S3 system has more silver atoms than the other, it has more sources to generate dislocations during the plastic regime. Therefore, silver atoms decrease the yield strength of copper, as well as increase the partial dislocation nucleation. However, it must be emphasized that in order to determine the exact effect of silver impurities on the yield strength of copper, a thorough statistical study on different placements of silver atoms must be carried out.

3.4. Stress–strain relationships at different temperatures

To elucidate the effect of temperature on the Cu–Ag nanowires, the stress–strain curve, at 100 K and 300 K, is calculated for the Cu 0.0, 0.2 and 0.4 at.% Ag systems from Section 3.1. The curves are shown in Fig. 10(a) and (b) for 100 K and 300 K respectively. As it can be seen, the yield strength of the systems decreases as the temperature increases. Furthermore, the silver impurities are seen again to modify the yield strength, decreasing its value compared to the impurity free system. However, similar as it was discussed in Section 3.3, a statistical study on different samples must be carried out in order to clarify the effect of temperature and silver

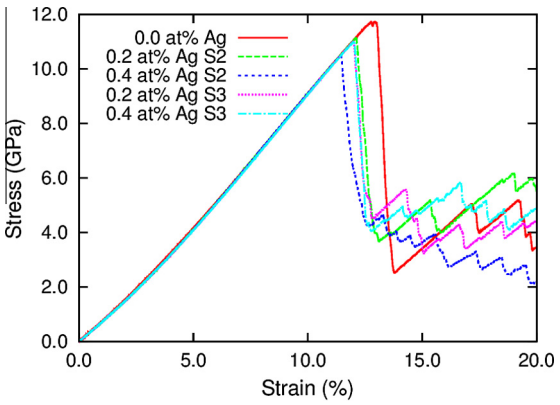

Fig. 9. Stress–strain relationships for different samples and concentrations of the Cu–Ag system.

Table 3
Yield strain and yield stress for different Cu–Ag samples.

Ag content (at.%) and sample	Yield strain (%)	Yield stress (GPa)
0.0	12.9	11.7
0.2 S2	12.1	11.1
0.4 S2	11.5	10.5
0.2 S3	12.0	11.1
0.4 S3	12.0	11.0

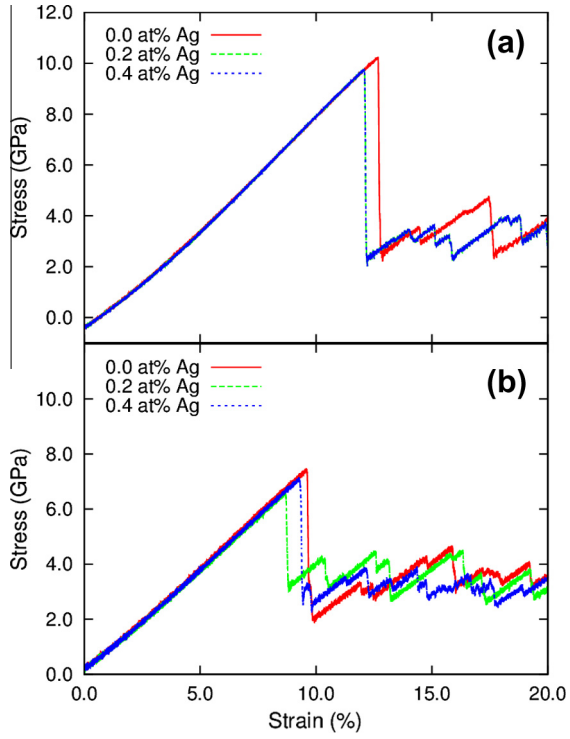

Fig. 10. Stress–strain relationships for the Cu–Ag system at (a) 100 K and (b) 300 K.

atoms on the yield strength of copper nanowires. It is important to note that atoms are subjected to thermal vibrations. Therefore, since the virial stress considers the kinetic energy of atoms and the temperatures here are 100 K and 300 K, the initial stress of these systems is not zero.

4. Conclusions

Silver impurities are found to promote partial dislocation nucleation, lowering both the yield stress and yield strain of single crystal copper nanowires along ⟨100⟩ loading direction, for all the concentrations studied here. Further, the yield point decreases with the presence of Ag atoms. The reason of this phenomenon is that because the size mismatch between silver and copper atoms, a local stress field appears, reducing the unstable stacking fault energy, which in turn promotes the nucleation and the propagations of the partial dislocations. However, the reduction of energy is, in general, tiny, resulting the dislocation nucleation from a competition of impurities and defects generated after the first partial dislocation is emitted. Also, it is possible to predict, in principle, the effect of other impurities using these results. According to the literature (see for example Schweinfest et al. [16]) the two main characteristics that define the effect of an impurity are the electronic structure of the atoms and its radius. In this sense, Ag, Au and Ni are similar. Therefore, Au and Ni should decrease slightly the unstable stacking fault energy of copper, promoting partial dislocation nucleation as Ag does. On the other hand, for example, Bi and Pb have similar electronic structure and atomic radius and very different from Cu, therefore their effects are completely different from Ag, Au, or Ni impurities. However, it is hard to determine 'a priori' the exact effect of impurities on the mechanical behaviour of copper.

The competition for partial dislocation nucleation between silver impurities and defects, after the emission of the first partial is also expected when the sample size is increased. Although the free surface will compose a smaller fraction of the system, the dislocations will still nucleate from there as well as from silver impurities, because the required energy is lower, compared to the required energy for nucleating from the bulk.

Finally, it was found that the yield strength of the material decreases when the temperature increases. Furthermore, the presence of silver impurities also decreases the yield strength compared to the impurity free system. However, a thorough and carefully statistical study is required in order to understand the complete effect of silver impurities on the transition from elastic to plastic behaviour of copper nanowires at different temperatures.

Acknowledgments

This work is supported by a Codelco-IM2 Grant. NA thanks Conicyt fellowship and GG acknowledges partial support from Fondecyt-Chile 1120603.

References

[1] M.H. Huang, S. Mao, H. Feick, H. Yan, Y. Wu, H. Kind, E. Weber, R. Russo, P. Yang, Science 292 (2001) 1897–1899.
[2] V. Rodrigues, D. Ugarte, Phys. Rev. B 63 (2001) 073405.
[3] X. Duan, Y. Huang, R. Agarwal, C.M. Lieber, Nature 421 (2003) 241–245.
[4] A. Husain, J. Hone, H.W.C. Postma, X.M.H. Huang, T. Drake, M. Barbic, A. Scherer, M.L. Roukes, Appl. Phys. Lett. 83 (2003) 1240–1242.
[5] H.W.C. Postma, I. Kozinsky, A. Husain, M.L. Roukes, Appl. Phys. Lett. 86 (2005) 223105.
[6] H. Liu, J. Kameoka, D.A. Czaplewski, H.G. Craighead, Nano Lett. 4 (2004) 671–675.
[7] T. Zhu, J. Li, K.J.V. Vliet, S. Ogata, S. Yip, S. Suresh, J. Mech. Phys. Solids 52 (2004) 691–724.
[8] M.A. Tschopp, D.E. Spearot, D.L. McDowell, Modell. Simul. Mater. Sci. Eng. 15 (2007) 693.
[9] J. Schitz, K.W. Jacobsen, Science 301 (2003) 1357–1359.
[10] H.V. Swygenhoven, J.R. Weertman, Mater. Today 9 (2006) 24–31.
[11] P. Heino, H. Häkkinen, K. Kaski, Phys. Rev. B 58 (1998) 641–652.
[12] S. Traiviratana, E.M. Bringa, D.J. Benson, M.A. Meyers, Acta Mater. 56 (2008) 3874–3886.
[13] K. Zhao, C. Chen, Y. Shen, T. Lu, Comput. Mater. Sci. 46 (2009) 749–754.
[14] E.M. Bringa, S. Traiviratana, M.A. Meyers, Acta Mater. 58 (2010) 4458–4477.
[15] Y.T. GU, H.F. ZHAN, Int. J. Comput. Methods 09 (2012) 1240003.
[16] R. Schweinfest, A. Paxton, M. Finnis, Nature 432 (2004) 1008–1011.
[17] P.C. Millett, R.P. Selvam, A. Saxena, Mater. Sci. Eng.: A 431 (2006) 92–99.
[18] R.K. Rajgarhia, D.E. Spearot, A. Saxena, Modell. Simul. Mater. Sci. Eng. 17 (2009) 055001.
[19] R.K. Rajgarhia, D.E. Spearot, A. Saxena, J. Mater. Res. 25 (2010) 411–421.
[20] H. Ikeda, Y. Qi, T. Çagin, K. Samwer, W.L. Johnson, W.A. Goddard, Phys. Rev. Lett. 82 (1999) 2900–2903.
[21] H.S. Park, J.A. Zimmerman, Phys. Rev. B 72 (2005) 054106.
[22] Y. Gao, H. Wang, J. Zhao, C. Sun, F. Wang, Comput. Mater. Sci. 50 (2011) 3032–3037.
[23] H. Zhan, Y. Gu, C. Yan, X. Feng, P. Yarlagadda, Comput. Mater. Sci. 50 (2011) 3425–3430.
[24] G. Tréglia, B. Legrand, J. Eugène, B. Aufray, F. Cabané, Phys. Rev. B 44 (1991) 5842–5854.
[25] M. Menyhard, M. Yan, V. Vitek, Acta Metall. Mater. 42 (1994) 2783–2796.
[26] J. Creuze, F. Berthier, R. Tétot, B. Legrand, Phys. Rev. B 62 (2000) 2813–2824.
[27] P. Subramanian, J. Perepezko, J. Phase Equilib. 14 (1993) 62–75.
[28] S. Plimpton, J. Comput. Phys. 117 (1995) 1–19.
[29] A. Stukowski, Modell. Simul. Mater. Sci. Eng. 18 (2010) 015012.
[30] P.L. Williams, Y. Mishin, J.C. Hamilton, Modell. Simul. Mater. Sci. Eng. 14 (2006) 817.
[31] Y. Mishin, M.J. Mehl, D.A. Papaconstantopoulos, A.F. Voter, J.D. Kress, Phys. Rev. B 63 (2001) 224106.
[32] M.S. Daw, M.I. Baskes, Phys. Rev. B 29 (1984) 6443–6453.
[33] C.L. Kelchner, S.J. Plimpton, J.C. Hamilton, Phys. Rev. B 58 (1998) 11085–11088.

[34] Here we use a single realization for each system, because we are mainly interested in the mechanism of dislocation emission rather than the general effect of impurities or the temperature on the yield point. Nevertheless, to explore the latter point, we perform simulations with two more different realizations and at two different temperatures, which are discussed in Sections 3.3 and 3.4, respectively.
[35] J.A. Zimmerman, H. Gao, F.F. Abraham, Modell. Simul. Mater. Sci. Eng. 8 (2000) 103.